ISSN 1070-3632, Russian Journal of General Chemistry, 2015, Vol. 85, No. 4, pp. 882–888. © Pleiades Publishing, Ltd., 2015.
Original Russian Text © O.E. Zhuravlev, A.Yu. Karpenkov, D.Yu. Karpenkov, L.I. Voronchikhina, 2015, published in Zhurnal Obshchei Khimii, 2015, Vol. 85, No. 4, pp. 641–647.

Composition and Structure of the Incombustible Residue from Thermal Decomposition of the Ionic Liquid *N*-Decylpyridinium Tetrachloroferrate(III)

O. E. Zhuravlev, A. Yu. Karpenkov, D. Yu. Karpenkov, and L. I. Voronchikhina

Tver State University, Sadovyi per. 35, Tver, 170002 Russia
e-mail: pifchem@mail.ru

Received December 23, 2014

Abstract—A low-temperature ionic liquid, *N*-decylpyridinium tetrachloroferrate(III), has been synthesized, and its thermal stability in air has been studied by thermogravimetry. Combustion of the organic part of this ionic liquid leaves a solid residue which has been studied by elemental analysis, X-ray powder diffraction, scanning electron microscopy, IR spectroscopy, and magnetometry. The incombustible residue has been identified as hematite (crystalline α-Fe_2O_3) which is a weak ferromagnetic at room temperature.

Keywords: ionic liquids, synthesis, thermal stability, hematite, thermal decomposition, magnetic properties
DOI: 10.1134/S1070363215040209

In recent years, the number of reviews, original articles, and patents dealing with various aspects of the preparation and application of ionic liquids has increased considerably [1]. Ionic liquids are substances that are liquid at temperatures below 100°C; they consist of bulky organic cations and various organic or inorganic anions. Some ionic liquids have already found application in different industries, in particular as catalysts and in the manufacture of polymeric and composite materials, high-capacity rechargeable batteries, condensers, etc. [2–10]. A number of ionic liquids are produced on a small scale by foreign companies.

The nature of the anion strongly affects such properties of ionic liquids as melting point, viscosity, density, and others. If the anion is a transition metal halide (Fe, Co, Ni, Mn, etc.) possessing paramagnetic properties, such ionic liquids are sensitive to magnetic field (i.e., exhibit magnetic susceptibility).

In 2004, Hayashi and Hamagushi [11] synthesized magnetic ionic liquids on the basis of 1,3-dialkylimidazolium and tetrachloroferrate as anion; their magnetic properties were determined by the presence of a high spin $FeCl_4^-$ ion. However, the term "magnetic ionic liquids" should be regarded as arbitrary since real magnetic liquids are characterized by several orders of magnitude higher magnetic susceptibility, so that the term "paramagnetic ionic liquids" is more appropriate.

We previously studied the thermal stability of some 1,3-dialkylimidazolium, *N*-alkylpyridinium, and tetraalkylammonium tetrachloroferrates [12, 13]. In all cases, thermal decomposition tetrachloroferrates during thermogravimetric analysis in the temperature range from 25 to 900°C left an undecomposable residue, assumingly iron oxide. Thermal decomposition of tetrabutylammonium [14] and quinolinium tetrachloroferrates [15] was studied. Volatile decomposition products were analyzed by mass spectrometry, but no analysis of the solid residue was performed, which would favor deeper understanding of the mechanism of decomposition.

We analyzed the residue obtained after thermal decomposition of *N*-decylpyridinium tetrachloroferrate(III) at different temperatures with the goal of determining its composition and structure. *N*-Decylpyridinium tetrachloroferrate(III) was synthesized by reaction of accessible *N*-decylpyridinium chloride with iron(III) chloride in acetone (Scheme 1). The main characteristics of this ionic liquid are as follows: molecular weight *M* 418.03; viscosity $\eta_{25°C}$ = 719.5 mPa s, $\eta_{65°C}$ = 205.3 mPa s; density d^{25} = 1.636 g/cm^3, d^{65} = 1.597 g/cm^3; decomposition point 360°C.

The IR spectrum of *N*-decylpyridinium tetrachloroferrate(III) in the range from 400 to 4000 cm^{-1} (Fig. 1)

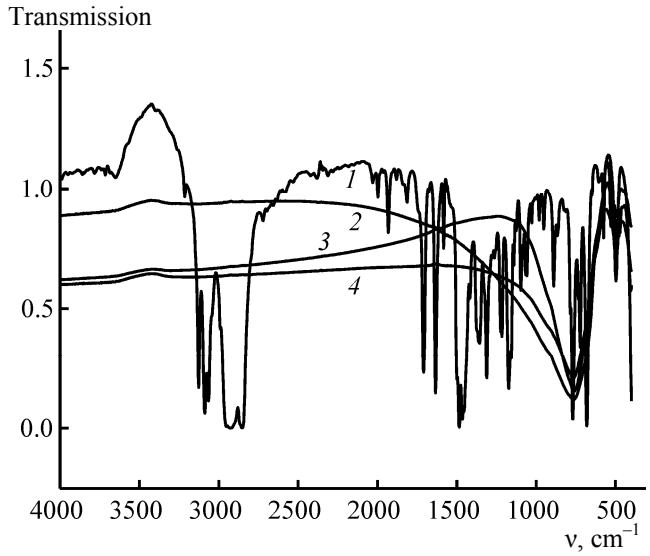

Fig. 1. IR spectra of (*1*) *N*-decylpyridinium tetrachloroferrate(III) and reduces obtained after its thermal decomposition at (*2*) 500, (*3*) 700, and (*4*) 900°C.

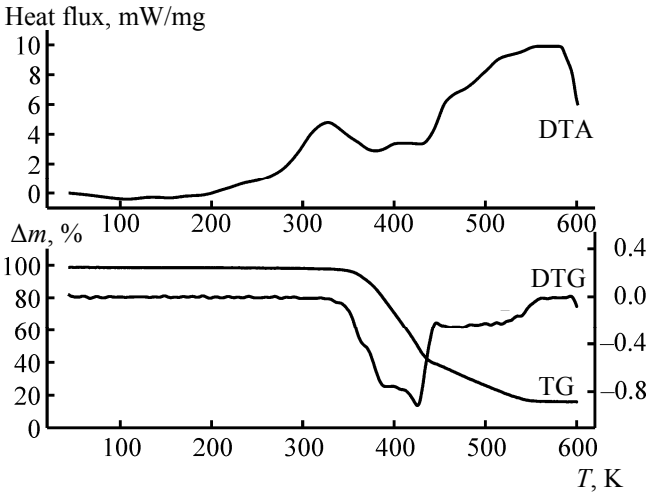

Fig. 2. DTA, DTG, and TG curves of *N*-decylpyridinium tetrachloroferrate(III).

confirms its structure. Its electronic absorption spectrum in acetone contains three maxima in the visible region at λ 534, 619, and 688 nm due to electron transitions in the tetrahedral tetrachloroferrate ion [11].

The IR spectrum of the solid residue lacked absorption bands assignable to organic fragment, indicating its inorganic nature. At a temperature of 500°C and higher, gaseous decomposition products burn in air, as follows from the exothermic effect at 550°C and the absence in the IR spectrum of absorption bands due to stretching vibrations of C–H_{arom} (3100–3000 cm^{-1}), C–H_{aliph} (3000–2850 cm^{-1}), and C=C_{arom} bonds (1600–1450 cm^{-1}) (Fig. 1).

The thermogravimetric data obtained in the temperature range from 25 to 600°C in air showed a fairly high thermal stability of *N*-decylpyridinium tetrachloroferrate(III) compared to halide salts [13] (Fig. 2). The ionic liquid is stable up to 360°C, and it decomposes in the range 360–540°C. The first decomposition step (360–430°C) is accompanied by 60% weight loss. In the second step (430–540°C) the weight loss is 20%. At 550°C, the undecomposable residue is 20%.

We analyzed the residues obtained after combustion of samples of the ionic liquid in a muffle furnace in air at 500, 700, and 900°C over a period of 30 min. For comparison, we also examined the incombustible product of thermal decomposition of that sample of iron(III) chloride which was used for the synthesis of *N*-decylpyridinium tetrachloroferrate(III). In all cases, the residues were fine black powders whose elemental composition conformed to iron(III) oxide.

Figure 3 shows the SEM image of samples obtained after thermal decomposition of the ionic liquid and iron(III) chloride. It is seen that combustion of the ionic liquid at 700°C yields mainly octahedral particles with a size of 5–10 μm (Figs. 3a, 3b). The decomposition of $FeCl_3$ at the same temperature produces smaller particles (2–5 μm) with preferentially cubic shape (Figs. 3c, 3d). In both cases, the products are Fe_2O_3 crystals with a fairly high symmetry. Combustion of the ionic liquid at 500°C gives irregularly shaped particles, whereas at 900°C iron(III) oxide is formed as 5–10-μm plates.

It is known that iron(III) oxide exists as several phases (α-, β-, γ-, and ε-Fe_2O_3) [16]. The samples of Fe_2O_3 obtained by thermal decomposition of the ionic

Scheme 1.

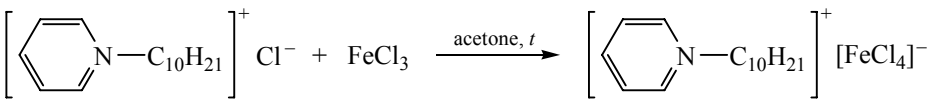

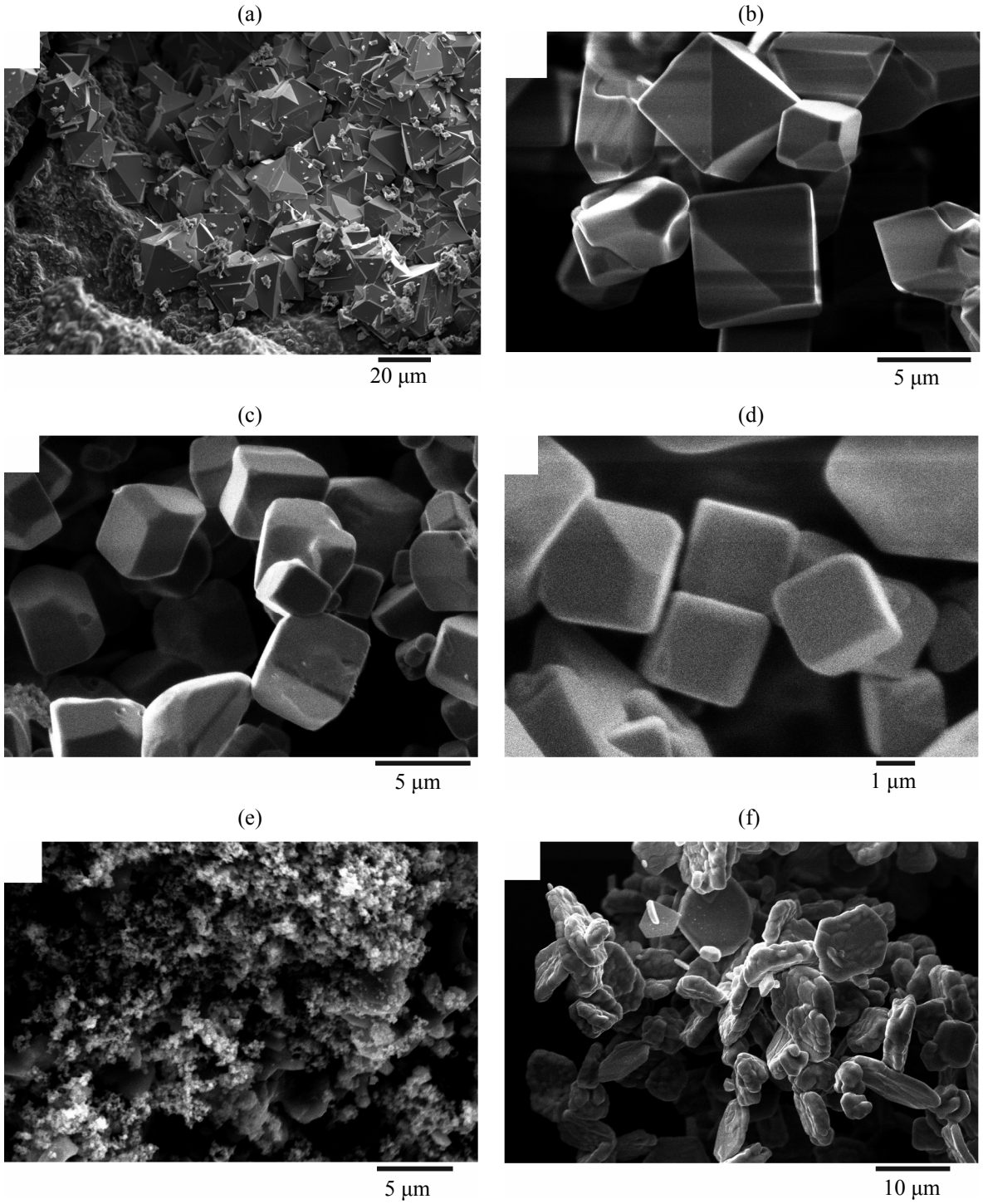

Fig. 3. SEM Image of iron(III) oxide crystals obtained after thermal decomposition of (a, b) *N*-decylpyridinium tetrachloroferrate(III) at 700°C, (c, d) iron(III) chloride at 700°C, and *N*-decylpyridinium tetrachloroferrate(III) at (d) 500 and (e) 900°C.

liquid at 500, 700, and 900°C and of iron(III) chloride at 700°C were subjected to X-ray powder diffraction (XRD) analysis. The results are shown in Fig. 4. The XRD patterns were obtained with 10% of zinc as internal standard. All samples are characterized by the same diffraction maxima whose position corresponds to the most stable iron(III) oxide polymorph, α-Fe_2O_3 (hematite, trigonal crystal lattice, $D_{3d}^6 R\bar{3}c$ symmetry)

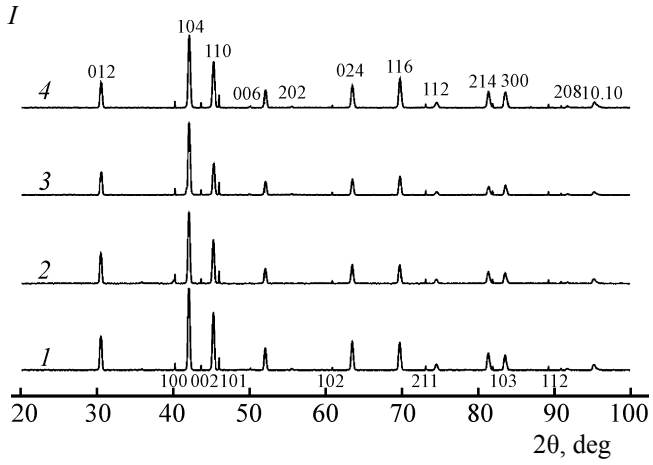

Fig. 4. X-Ray powder diffraction patterns of iron(III) oxide obtained after thermal decomposition of (*1*) iron(III) chloride at 700°C and *N*-decylpyridinium tetrachloroferrate(III) at (*2*) 500, (*3*) 700, and (*4*) 900°C.

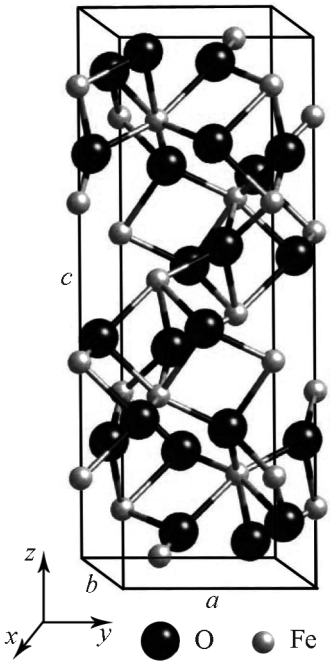

Fig. 5. Crystal structure of α-Fe_2O_3.

[16] (Fig. 5), and ZnO [zincite, hexagonal crystal structure, space group *P*6(3)/*mc*].

The unit cell parameters of Fe_2O_3 samples obtained at different temperatures together with published data are given in table. The sample obtained from iron(III) chloride is characterized by the largest unit cell parameters. The size of the Fe_2O_3 unit cell decreases as the combustion temperature rises. It should be noted that even a small difference in unit cell dimensions could give rise to essential variation of the physical properties of hematite [16].

We also determined the magnetization (M) in a magnetic field of 1.5 T, coercivity (H_c), and antiferromagnetic transition temperature (T_M) of the above samples (see table). Hematite at room temperature is a weak ferromagnetic with a ferromagnetic–paramagnetic transition temperature of 956 K. In fact, being an antiferromagnetic with disordered magnetic moments of the constituent sublattices, hematite acquires purely antiferromagnetic ordering at 260 K (Morin's temperature T_M) [17].

The basal plane of hematite (x–y plane in Fig. 5) includes two deeply penetrating antiferromagnetic Fe^{3+} sublattices. Insofar as the overall magnetic moments of these sublattices are not strictly antiparallel with a disorientation angle of less than 0.1°, hematite exhibits a weak ferromagnetism (Fig. 6). The phase transition at the temperature T_M involves reorientation of the sublattice magnetic moments from the basal plane to a direction inclined to the c axis by an angle of 7° (Fig. 6) [17, 18]; as a result, the sublattice magnetic moments become strictly antiparallel, and hematite acquires antiferromagnetic properties.

Figure 7 shows the magnetization and demagnetization curves for the examined samples at 300 K. In all cases, a hysteresis with a width of ~60–130 mT is observed. Taking into account that all samples at room temperature are weak ferromagentics, magnetic saturation cannot be achieved, and their magnetization linearly increases in magnetic field of higher than 0.5 T.

The stepwise change of the magnetization, which is seen most clearly for the sample obtained from the ionic liquid at 900°C (Fig. 7d), is likely to be related to the presence of a small amount (<0.5%) of a ferromagnetic impurity. This is confirmed by the temperature dependence of magnetization in a magnetic field of 1.5 T (Fig. 6). The transition from weak ferromagnetic ordering to antiferromagnetic is observed near 245 K; however, the magnetization remains nonzero below 200 K.

EXPERIMENTAL

***N*-Decylpyridiniyum tetrachloroferrate(III).** A mixture of acetone solutions of 0.05 mol of iron(III)

Crystal lattice parameters and magnetic properties of Fe_2O_3 samples

Initial compound	Combustion temperature, °C	Unit cell parameters			M ($\mu_0 H$ = 1.5 T), A m^2 kg^{-1}	$\mu_0 H_c$, mT	T_M, K
		a, Å	b, Å	c, Å			
Iron(III) chloride	700	5.0356	5.0356	13.7508	0.6	62	248
Ionic liquid	500	5.0322	5.0322	13.7378	0.55	131	247.4
	700	5.0294	5.0294	13.7252	0.59	62	247.6
	900	5.0293	5.0293	13.7182	0.67	89	243.5
α-Fe_2O_3 [16]	–	5.0342	5.0342	13.7483	0.55	500	265

chloride and 0.05 mol of *N*-decylpyridinium chloride was heated for 10–15 min under reflux with stirring. The solvent was removed, and the residue was dried for 24 h under reduced pressure over P_4O_{10}. The product was a dark green liquid soluble in water (highly hydrolyzable due to instability of $FeCl_4^-$ ion in aqueous medium) and other polar solvents (ethanol, acetone, acetonitrile). Yield 95%. IR spectrum (KBr), ν, cm^{-1}: 3055 (C–H_{arom}), 2978, 2843 (C–H_{aliph}), 1648 (C–C_{arom}), 1515, 1458 (C–C_{aliph}), 765, 680 (δ C–H_{aliph}). Found, %: C 43.3; H 6.5; N 3.5. $C_{15}H_{26}Cl_4FeN$. Calculated, %: C 43.1; H 6.3; N 3.4.

The IR spectra were recorded on an ALPHA spectrometer from thin film placed between KBr plates. The electronic absorption spectra in the visible region were measured on an SF-56 spectrophotometer (LOMO) from solutions in acetone (cell path length 1 cm). The microphotographs were obtained using a JEOL JSM 6490 LV scanning electron microscope. Thermogravimetric analysis was performed on a Netzsch STA 449 F3 instrument in a stream of air (temperature range 25–550°C, heating rate 5 deg/min). The elemental composition of the ionic liquid was determined on a Hewlett Packard 185 analyzer. The elemental analyses of the thermal decomposition products were obtained using a JEOL JSM 6490 LV scanning electron microscope equipped with an energy dispersive X-ray analyzer and a semiconductor detector; the results of 3–5 measurements were averaged.

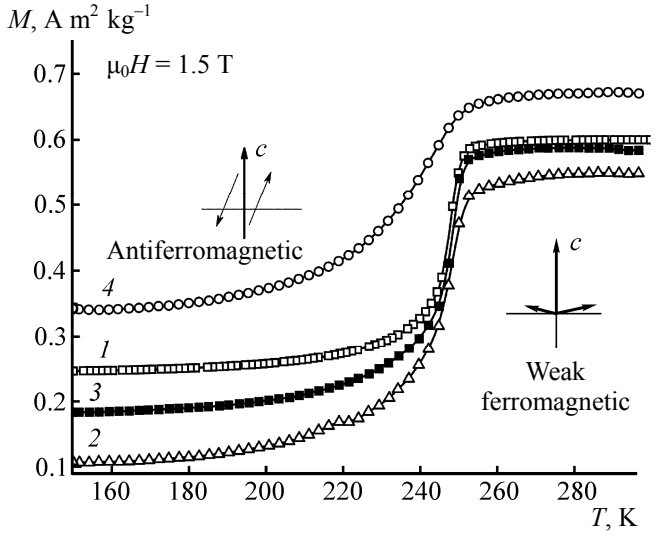

Fig. 6. Temperature dependences of the magnetization of iron(III) oxide obtained after thermal decomposition of (*1*) iron(III) chloride at 700°C and *N*-decylpyridinium tetrachloroferrate(III) at (*2*) 500, (*3*) 700, and (*4*) 900°C.

The X-ray diffraction patterns of powder samples were obtained on a DRON-6.0 diffractometer (FeK_α radiation, λ = 0.193735 nm) with a fixed focusing slit system. The unit cell parameters were determined from reflections measured in the range 20° < 2θ < 100° with a step of 0.01°. Samples were prepared by grinding with 10% of ZnO as internal standard and were stuffed into cells without pressing while continuously monitoring the surface quality to obtain maximally disordered specimens. The composition was determined by comparing the experimental and standard spectra. Quantitative analysis implied full-profile analysis of XRD patterns of the disoriented sample [19]. The addition of well-crystallized zincite (ZnO, 10%) as internal standard is necessary while analyzing amorphous and ill-crystallized phases.

The magnetization of samples was measured on a PPMS-14 Quantum Design vibration magnetometer utilizing the continuous induction method which is based on the interaction of alternating magnetic field of a vibrating sample with a static coil system. A

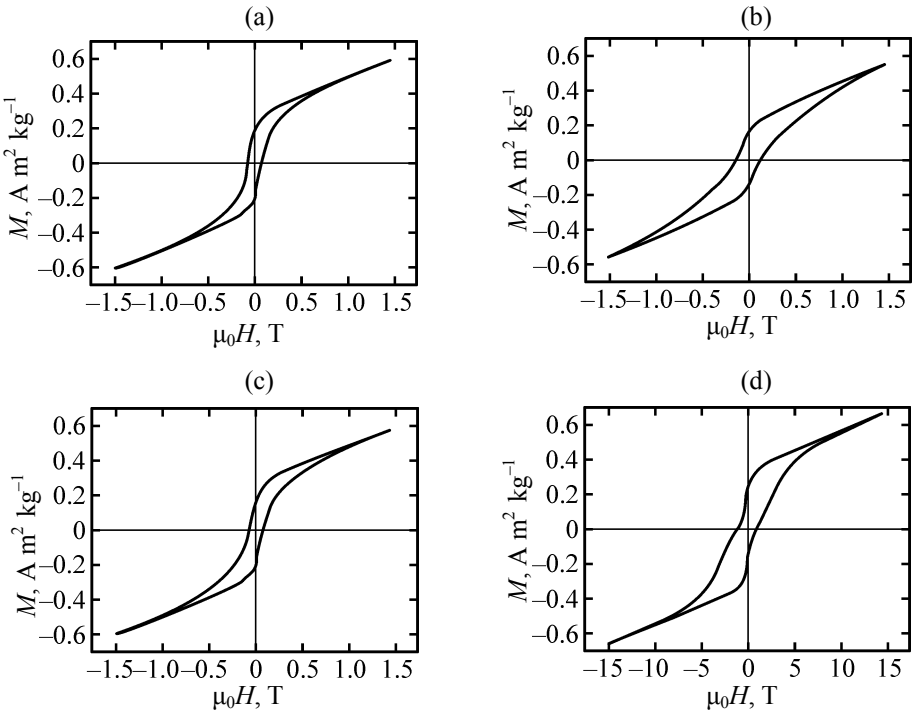

Fig. 7. Magnetic field dependences of the magnetization of iron(III) oxide obtained after thermal decomposition of (a) iron(III) chloride at 700°C and *N*-decylpyridinium tetrachloroferrate(III) at (b) 500, (c) 700, and (d) 900°C.

compact gradiometric configuration of the pickup coil with a relatively large vibration amplitude (1–3 mm) and a peak frequency of 40 Hz ensures magnetization measurement with an accuracy of less than 10^{-6} A m^2 at a data transfer rate of 1 Hz.

Thermogravimetric analysis was performed at the Physicochemical Analysis Department of the Shared Use Center of the Tver State University.

ACKNOWLEDGMENTS

This study was performed under financial support by the Ministry of Education and Science of the Russian Federation in the framework of a state research contract and by the President of the Russian Federation (program for state support of young Russian scientists, candidates of science; project no. 14.Z56.15.4358-MK).

REFERENCES

1. Vygodskii, Ya.S., Lozinskaya, E.I., and Shaplov, A.S., *Ros. Khim. Zh.*, 2004, vol. 68, no. 6, p. 40.
2. Gordon, S., *Appl. Catal.*, 2001, vol. 222, p. 101. DOI: 10.1016/S0926-860X.
3. Zhao, D., Wu, M., Kou, Y., and Min, E., *Catal. Today*, 2002, vol. 74, p. 157. DOI: 10.1155/2014/729842.
4. Sun, X. and Zhao, S., *Chin. J. Chem. Eng.*, 2006, vol. 14, p. 289. DOI: 10.1016/S1004-9541(06)60073-6.
5. Yong, W. and Hong, Y., *Chem. Eng. J.*, 2009, vol. 147, p. 71. DOI: 10.1016/j.cej.2008.11.043.
6. Xiaowei, P., Ye, H.Y., Liangyu, Y., Pan, Y., Junling, W., Rong, X., and Mary, B.Ch.-P., *Carbon*, 2010, vol. 48, p. 2501. DOI: 10.1016/j.carbon.2010.03.023.
7. Liang, L., Yu, H., Guoping, Y., Fangjun, L., Zhiliang, H., and Zhibin, M., *Mater. Lett.*, 2009, vol. 63, p. 8. DOI: 10.1016/j.matlet.2008.08.016.
8. Rezaei, B., Mallakpour, S., and Taki, M., *J. Power Sources*, 2009, vol. 187, p. 605. DOI: 10.4061/2011/787905.
9. Borgel, V., Markevich, E., Aurbach, D., Semrau, G., and Schmidt, M., *J. Power Sources*, 2009, vol. 189, p. 331. DOI: 10.1016/j.jpowsour.2008.08.099.
10. Di, W. and Tin, W.N., *Electrochem. Commun.*, 2009, vol. 11, p. 1996. DOI: 10.1016/j.elecom.2009.08.037.
11. Hayashi, S. and Hamagushi, H., *Chem. Lett.*, 2004, vol. 33, p. 1590. DOI: 10.1002/chin.200518200.
12. Zhuravlev, O.E., Verolainen, N.V., and Voronchikhina, L.I., *Russ. J. Appl. Chem.*, 2011. vol. 84, no. 7, p. 1158. DOI: 10.1134/S1070427211070068.

13. Zhuravlev, O.E., Nikol'skii, V.M., and Voronchikhina, L.I., *Russ. J. Gen. Chem*., 2014, vol. 84, no. 6, p. 1141. DOI: 10.1134/S1070363214060152.
14. Wyrzykowski, D., Maniecki, T., Pattek-Janczyk, A., Stanek, J., and Warnke, Z., *Thermochim. Acta*, 2005, vol. 435, p. 92. DOI: 10.1016/j.tca.2005.05.007.
15. Wyrzykowski, D., Pattek-Janczyk, A., Maniecki, T., Zaremba, K., and Warnke, Z., *Thermochim. Acta*, 2006, vol. 443, p. 72. DOI: 10.1016/j.tca.2005.12.023.
16. Schwertmann, U. and Cornell, R.M., *The Iron Oxides: Structure, Properties, Reactions, Occurrences and Uses*, Weinheim: Wiley–VCH, 2003.
17. Morish, A.H., Johnston, G.B., and Curry, N.A., *Phys. Lett*., 1963, vol. 7, p. 177. DOI: 10.1016/0031-9163(63)90372-X.
18. Artman, J.O., Murphy, J.C., and Foner, S., *Phys. Rev*., 1965, vol. 138, p. 912. DOI: 10.1103/PhysRev.138.A912.
19. Pushcharovskii, D.Yu., *Rentgenografiya mineralov* (X-Ray Diffraction of Minerals), Moscow: Geoinformmark, 2000.